



Seismotectonic Properties and Zonation of the Far-Eastern Eurasian Plate Around the Korean Peninsula

TAE-KYUNG HONG,¹ SEONGJUN PARK,¹ and SOUNG EIL HOUNG¹

Abstract—Regional seismotectonics provides crucial information for seismic hazard analysis, which is difficult to address with short-term earthquake records. The far-eastern Eurasian plate around the Korean Peninsula presents a stable intraplate environment with diffuse seismicity, of which responsible tectonics and active faults are difficult to identify. Combined analysis of instrumental and historical earthquake records is required for assessment of long-term seismicity properties. Seismotectonic provinces are identified from the spatial distribution of seismicity properties controlled by the medium properties and stress field. The boundaries of the seismotectonic provinces are defined considering the medium properties that can be inferred from geological, geophysical and tectonic features. The Gutenberg–Richter frequency–magnitude relationships and maximum magnitudes for the seismotectonic provinces are determined using instrumental and historical earthquake records. The validity of maximum magnitude estimation is tested with synthetic data. A parametric method, the Tate–Pisarenko method, produces more accurate estimates than non-parametric methods. A modified Tate–Pisarenko method is proposed for estimation of maximum magnitudes for incomplete short-term earthquake catalogs. The maximum magnitude of events for the whole region is approximately the same as the average of the maximum magnitudes of events for subdivided provinces, causing apparent variation in maximum magnitudes depending on the number of seismotectonic provinces. Consideration of a reasonable number of seismotectonic provinces may be needed for proper assessment of seismic hazard potentials is recommended. The combined analysis of historical and instrumental earthquake records suggests maximum magnitudes greater than 7 around the peninsula.

Key words: Seismotectonics, seismotectonic province, intraplate region, Korean Peninsula, seismicity, maximum magnitude.

1. Introduction

The seismotectonics is a tectonic framework combining seismicity, geology and geophysical properties, which are useful for inference of seismic

hazard potentials (GASPARINI *et al.*, 1982; POWELL *et al.*, 1994; LAVECCHIA *et al.*, 1994, COSTA *et al.*, 1996; DE and KAYAL 2003). A region can be divided into seismotectonic provinces considering the seismotectonic properties that are represented by maximum magnitudes, earthquake occurrence rates and potential peak ground accelerations. Each seismotectonic province can be defined by its unique seismicity properties and tectonic environments (CORNELL 1968). Seismotectonic province models have been proposed for a number of regions (NOWROOZI 1976; TAVAKOLI and GHAFORY-ASHTIANY 1999; MELETTI *et al.* 2000; SINGH *et al.* 2011). These regionalized provinces are used for seismic hazard analysis (e.g., FRANKEL 1995; MENON *et al.*, 2010). However, a routine procedure for constructing seismotectonic province models has not been established. Also, it remains unclear how many seismotectonic provinces are appropriate for each region.

It is difficult to assess the seismotectonic properties of low-seismicity intraplate regions with short seismic records. In particular, the intraplate regions adjacent to continental margins comprise paleo-tectonic structures that respond to the regional stress field (CHOI *et al.* 2012; HONG *et al.* 2015). The monitoring of seismogenic paleo-tectonic structures in oceanic regions by inland seismic networks can be poor. Also, tectonic-loading stress is accumulated slowly in intraplate regions, inducing destructive large earthquakes with long recurrence time intervals (e.g., TALWANI and COX 1985).

Seismicity with long recurrence intervals is limitedly observable in short-term earthquake catalogs. Long-term seismicity records may contribute to the assessment of potential seismic hazards. Historical earthquake records may be useful for long-term

¹ Department of Earth System Sciences, Yonsei University, 50 Yonsei-ro, Seodaemun-gu, Seoul 120-749, South Korea. E-mail: tkhong@yonsei.ac.kr

seismicity analysis. Thus, analysis of both instrumental and historical earthquake records may be desirable. However, historical earthquake records suffer from inherent incompleteness, and the source parameters are poorly constrained. Thus, it remains unclear how historical earthquake catalogs should be combined with instrumental earthquake catalogs for seismic hazard analysis. Also, the necessary time period of earthquake catalogs for seismic hazard analysis remains unclear.

We propose a seismotectonic province model for the Korean Peninsula that belongs to a stable intraplate regime where major earthquakes occur with long recurrence intervals. Seismotectonic province models based on both the tectonics and seismicity have been rarely proposed for the Korean Peninsula (e.g., KIM and LEE 2000). The early models generally resembled the geological province structures. In this study, the seismicity and geophysical properties, and geological and tectonic features are combined to determine the seismotectonic province models. Both the instrumental and historical earthquake records are combined for the analysis of seismicity properties and maximum magnitudes. The variation of seismicity properties and maximum magnitudes depending on the seismotectonic province model is investigated.

Also, the effect of seismotectonic province models on the determination of seismicity properties and maximum magnitudes is examined.

2. Geology and Tectonics

The Korean Peninsula is located in an intraplate region adjacent to the far-eastern Eurasian plate margin (Fig. 1). The far-eastern Eurasian plate converges with the Philippines Sea plate at the region off the southern Japanese islands, and with the Okhotsk plate at the eastern margin of the East Sea (Sea of Japan). The collisions of Eurasian plate inducing an tectonic-loading stress field composed of ENE-directional compression and WNW-directional tension around the Korean Peninsula (CHOI *et al.* 2012) (Fig. 1). The current appearance of the Korean Peninsula was formed by a continental collision between North China and South China blocks during late Permian to Jurassic, which was followed by a continental-rifting opening the East Sea (Sea of Japan) during the Oligocene to mid-Miocene (JOLIVET *et al.* 1994; CHOUGH *et al.* 2000; OH 2006). The continental collision developed a characteristic NE-trending geological provinces. The surface of the

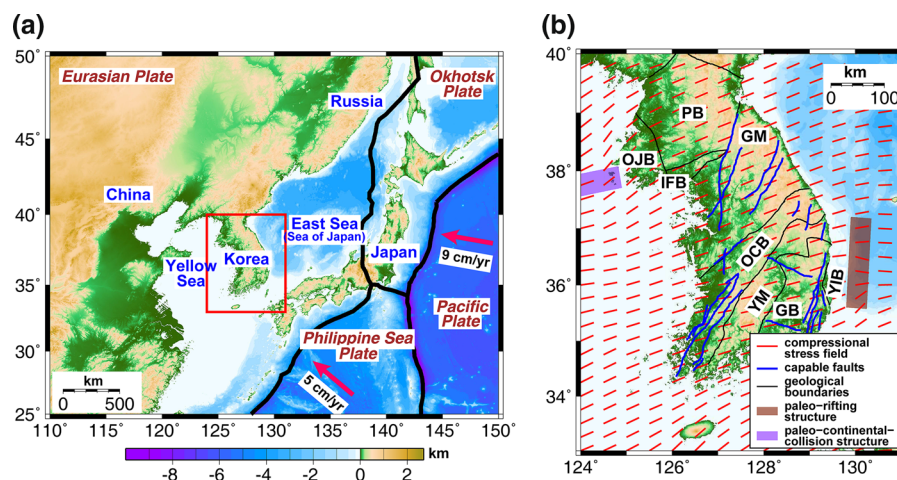


Figure 1

a Geological and tectonic structures around the Korean Peninsula (e.g., CHOUGH *et al.* 2000). **b** An enlarged map of the study region. The major geological provinces are denoted: GM Gyeonggi massif, GB Gyeongsang basin, IFB Imjingang fold belt, NM Nangrim massif, OCB Okcheon belt, OJB Ongjin basin, YM Yeongnam massif, YIB Yeonil basin (YIB). The ambient compression stress field (CHOI *et al.* 2012) and capable faults in the peninsula (CHOI 2012) are denoted. The regions of paleo-rifting in the East Sea and the paleo-continental-collision in the Yellow Sea are shaded

peninsula is composed of three precambrian massif blocks and two intervening belts (CHOUGH *et al.* 2000).

The paleo-continental-collision developed an EW-trending subparallel structures in the central Yellow Sea, which were reactivated by the ambient NS-directional tension and Ryukyu trench rollback and produce normal-faulting earthquakes (Fig. 1). Also, the paleo-rifting developed NS-trending offshore paleo-normal-faulting structures subparallel with the east coast of the peninsula. The paleo-normal-faulting structures were reactivated by the EW-directional lithostatic compression, producing thrustal earthquakes (CHOI *et al.* 2012). A solidified

underplated magma associated with the East Sea opening appears to be present in the lower crust off the east coast of the peninsula, which is illuminated by high Pn velocity, high magnetic anomalies and high V_P/V_S ratios (CHO *et al.* 2004; HONG and KANG 2009; JO and HONG 2013) (Fig. 2).

The massif blocks (Gyeonggi massif, Yeongnam massif) are illuminated as high seismic velocity regions (HONG and KANG 2009). Geophysical and seismic properties of the crust (crustal shear wave velocity, gravity anomaly, crustal P amplification, Lg Q , Pn tomography, heat flow) generally follow the geological structures in the surface (Fig. 2). The Pn seismic velocities are observed to be low along the

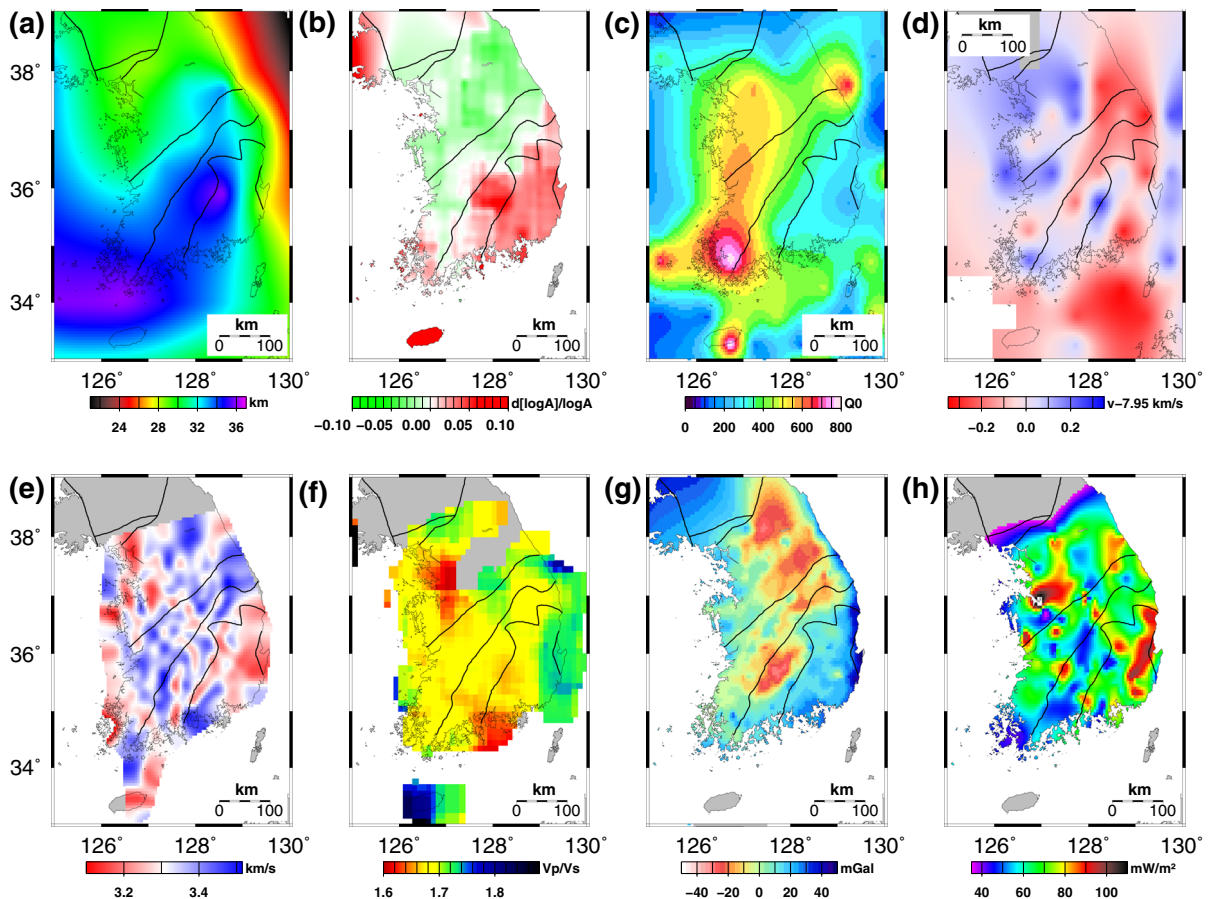


Figure 2

Regional variation in the seismic and geophysical properties of the crust of the Korean Peninsula: **a** crustal thickness (HONG *et al.* 2008), **b** crustal P amplification (HONG and LEE 2012), **c** crustally-guided shear-wave attenuation factors (Lg Q_0) (HONG and CHOI 2012), **d** Moho P (Pn) velocities (HONG and KANG 2009), **e** shear-wave velocities at a depth of 6.75 km (CHOI *et al.* 2009), **f** upper-crustal V_P/V_S ratios (JO and HONG 2013), **g** Bouguer gravity anomalies (CHO *et al.* 1997), and **h** heat flows (LEE *et al.* 2010).

east coast. The southeastern peninsula (Gyeongsang basin) is covered by Cretaceous volcanic sediments where high heat flows, low shear wave velocities, high gravity anomalies, low Pn velocities, low Lg Q , and high P amplification are observed.

The inland peninsula and Yellow Sea display typical features of continental crusts with thicknesses of 29–36 km (CHANG *et al.*, 2004; HONG *et al.* 2008; HE and HONG 2010). The paleo-continental-rifting developed transitional crusts between continental and oceanic crusts in the East Sea (Fig. 1). The crustal thicknesses in the East Sea decrease abruptly across the east coast, and reach 8.5–10 km in the Japan basin (HIRATA *et al.* 1992; KIM *et al.* 1998). Continental shelves cover the most regions of the Yellow Sea, while are extended only for several tens of kilometers in the East Sea. A number of faults were investigated (e.g., LEE and UM 1992; KYUNG 2003; LEE and YANG 2007). Only several faults were identified to be capable (CHOI 2012) (Fig. 1). The faults in the peninsula strike dominantly in NE, displaying acute angles to the ambient compressional stress field. These strikes of faults are consistent with the geometry of geological structures, which might result from the paleo-continental collision.

3. Seismicity and Earthquake Records

The instrumental seismic monitoring in the Korean Peninsula began in 1978, and the number of reported earthquakes until 2013 is 14,992 (Fig. 3). We collect the event information of the instrumentally-recorded earthquakes from the Korea Meteorological Administration (KMA), Japan Meteorological Agency (JMA), and China Earthquake Network Center (CENC). The largest magnitude of the instrumentally-recorded events is 5.3 (Fig. 4). Six earthquakes with magnitudes equal to or greater than 5.0 occurred in the Korean Peninsula since 1978. It is noteworthy that an M6.5 earthquake was reported to have occurred at the northwestern peninsula in 1952 (ENGDahl and VILLASENOR 2002). Most events occur at depths less than 20 km, and the largest focal depth is 35 km (Fig. 5).

Strike-slip earthquakes are dominant in the peninsula (Fig. 5). Characteristic normal-faulting earthquakes are observed around the paleo-continental collision belt in the central Yellow Sea (HONG and CHOI 2012). Thrust earthquakes occur along the NS-trending paleo-rifting structure off the east coast of the peninsula (CHOI *et al.* 2012). These normal-

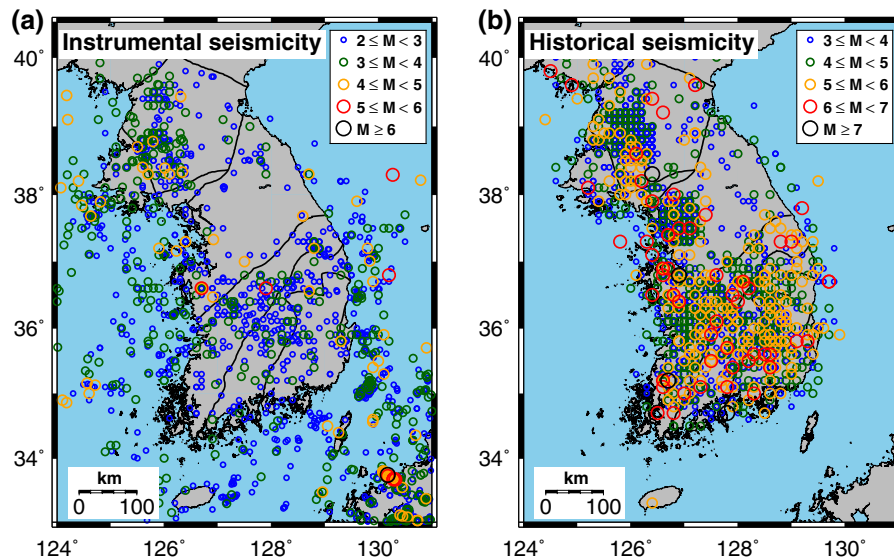


Figure 3

a Instrumental seismicity from 1978 to 2013 and **b** historical seismicity from 1393 to 1904 around the Korean Peninsula. Offshore events were recorded limitedly in the historical earthquake catalog. The spatial distribution of seismicity is similar between instrumental and historical earthquakes

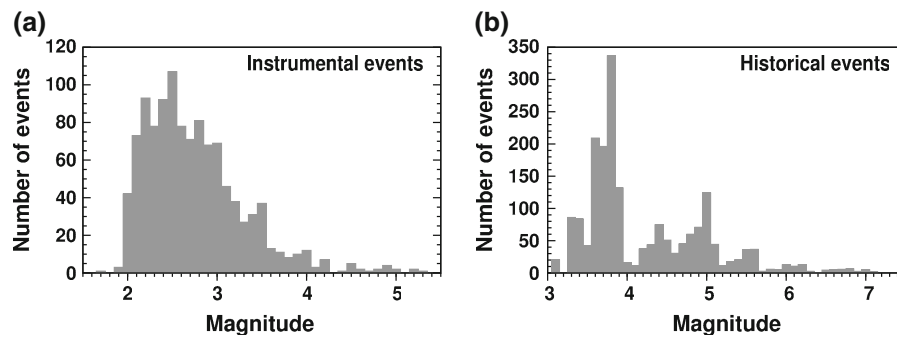


Figure 4

Distribution of earthquakes as a function of magnitude: **a** instrumental earthquakes and **b** historical earthquakes. Historical earthquakes with magnitudes of 4.0–4.5 appear to have been under-recorded

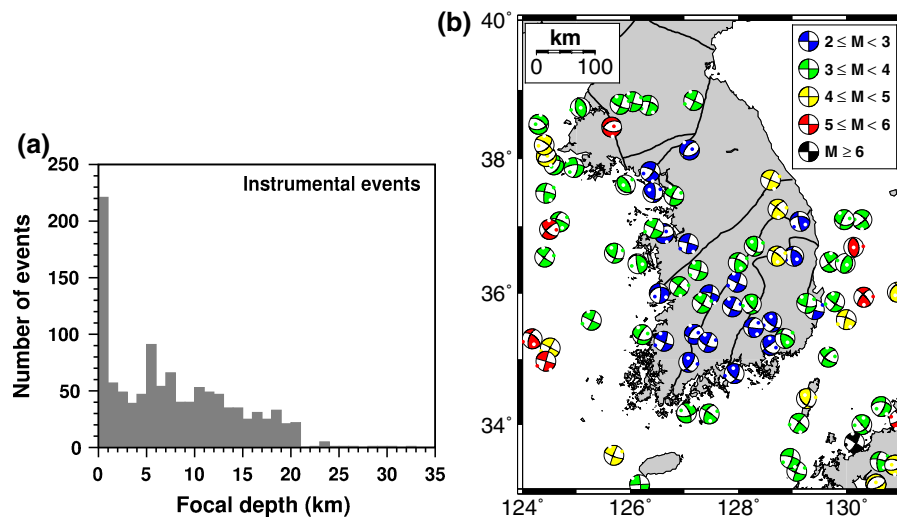


Figure 5

a Focal depth distribution of instrumental earthquakes. Most earthquakes occur at depths less than 20 km. **b** Focal mechanism solutions for earthquakes around the Korean Peninsula. Strike-slip earthquakes striking in NE are dominant around the peninsula. Reverse-faulting earthquakes striking in NS are observed in the region off the east coast of the peninsula, and normal-faulting earthquakes striking in EW are observed in the region around the northwestern peninsula

faulting and thrustal earthquakes result from the response of paleo-tectonic structures to the ambient stress field. It is observed that the instrumental seismicity is weakly correlated with known capable faults (cf., Figs. 1, 3)

The historical earthquake records are analyzed to reflect the seismicity with long recurrence time intervals. A number of historical earthquakes were recorded in historical literatures including Samgooksagi, Koryosa and Choseonwangjosillo. Some devastating earthquakes produced seismic damages

with seismic intensities of VIII in the modified Mercalli intensity (MMI) scale (LEE and YANG 2006). Most historical earthquakes were recorded during Joseon dynasty (1393–1904), and the number of events is 1893 (Figs. 3, 4). The event information for the historical earthquakes is collected from HOUNG and HONG (2013). However, the magnitudes of the historical earthquakes are re-determined based on a recently-developed magnitude–intensity relationship that is given by (PARK and HONG 2014):

$$I(M_L, l, h) = 1.72M_L - 0.322 \ln(l^2 + h^2) - 0.00608 \sqrt{l^2 + h^2} - 0.998, \quad (1)$$

where I is the seismic intensity in the MMI scale, M_L is the event magnitude in the local magnitude scale, h is the focal depth in kilometer, and l is the epicentral distance in kilometer.

4. Theory

4.1. Gutenberg–Richter Seismicity Constants

The minimum magnitude, M_{\min} , represents the threshold magnitude above which the event catalog is complete (e.g., RYDELEK and SACKS 1989; GOMBERG 1991). An earthquake catalog for events with magnitudes greater than M_{\min} generally satisfies the Gutenberg–Richter frequency–magnitude relationship:

$$\log N = a - bM, \quad (2)$$

where a and b are constants, M is the magnitude, and N is the number of events with magnitudes greater than or equal to M . The fitness between the seismicity data and theoretical curve is estimated by

$$R = 1 - \frac{\sum_{j=1}^n |B_j - S_j|}{\sum_{j=1}^n B_j}, \quad (3)$$

where B_j is the number of events with magnitudes greater than or equal to M_j , S_j is the reference value from the Gutenberg–Richter relationship, and n is the total number of events in the dataset. From Eq. (2), the Gutenberg–Richter b value for an event catalog with a minimum magnitude of M_{\min} satisfies (AKI 1965)

$$b = \frac{1}{\ln(10) \times (\bar{M} - M_{\min})}, \quad (4)$$

where \bar{M} is the average of the observed magnitudes.

If the magnitude-dependent earthquake distribution follows a probability density function, $f(m)$, the number of earthquakes (N) with magnitudes greater than or equal to M satisfies (TINTI and MULARGIA 1985)

$$\begin{aligned} N &= 10^a \int_M^\infty f(m) dm = 10^a \left[1 - \int_0^M f(m) dm \right] \\ &= 10^a [1 - F(M)], \end{aligned} \quad (5)$$

where the function $F(M)$ is the cumulative distribution function that is the integral function of $f(m)$. Function $F(M)$ is given by

$$F(M) = 1 - 10^{-bM}. \quad (6)$$

The probability density function, $f(M)$, is calculated by differentiating $F(M)$:

$$f(M) = \beta e^{-\beta M}, \quad (7)$$

where β is given by

$$\beta = b \ln(10). \quad (8)$$

The probability density function, $f(M)$, is normalized for events with magnitudes greater than or equal to M_{\min} . The normalized probability density function, $\hat{f}(M)$, is defined to be

$$\hat{f}(M) = \frac{\beta e^{-\beta M}}{\int_{M_{\min}}^\infty f(m) dm} = \beta e^{-\beta(M - M_{\min})}. \quad (9)$$

Hereafter, function $\hat{f}(M)$ is used for $f(M)$. The population mean ($E(M)$) and population variation ($\text{Var}(M)$) of magnitude distribution $f(m)$ are given by

$$\begin{aligned} E(M) &= \int_{M_{\min}}^\infty mf(m) dm = M_{\min} + \frac{1}{\beta}, \\ \text{Var}(M) &= \int_{M_{\min}}^\infty m^2 f(m) dm - [E(M)]^2 = \frac{1}{\beta^2}. \end{aligned} \quad (10)$$

Thus, an earthquake catalog with a sufficiently large number (n) of events displays a normal distribution with a mean of $M_{\min} + 1/\beta$ and variation of $1/(n\beta^2)$.

When the event catalog satisfies a normal distribution, the β estimate, $\hat{\beta}$, for an event catalog with mean magnitude of \bar{M} can be written as

$$\begin{aligned} \hat{\beta} &= \int_{-\infty}^\infty \beta \exp \left[-\frac{1}{2} \times \frac{\left\{ \bar{M} - \left(M_{\min} + \frac{1}{\beta} \right) \right\}^2}{\frac{1}{n\beta^2}} \right] d\beta \\ &= \frac{1}{\bar{M} - M_{\min}}. \end{aligned} \quad (11)$$

The b value based on the earthquake catalog is estimated to be

$$\hat{b} = \frac{\hat{\beta}}{\ln(10)} = \frac{1}{\ln(10)(\bar{M} - M_{\min})}. \quad (12)$$

The accuracy of the minimum magnitude (M_{\min}) is dependent on the magnitude precision in the catalog.

When the apparent minimum magnitude for an event catalog with a discrete magnitude interval of ΔM is given by M_{thre} , the practical minimum magnitude is given by

$$M_{\text{min}} = M_{\text{thre}} - \frac{\Delta M}{2}. \quad (13)$$

Thus, the b value for the earthquake catalog can be written as

$$\hat{b} = \frac{1}{\ln(10) \times [(M - (M_{\text{thre}} - \Delta M/2))].} \quad (14)$$

Also, the \hat{a} value for the event catalog is given by

$$\hat{a} = \log(N) + \hat{b}M_{\text{min}}. \quad (15)$$

4.2. Determination of Maximum Magnitude, M_{max}

The maximum magnitude, M_{max} , is the upper limit of event magnitudes that can occur in the given region (KIJKO and SINGH 2011). The maximum magnitudes can be estimated deterministically based on empirical relationships between magnitudes and fault parameters (e.g., WELLS and COPPERSMITH 1994). Also, numerous probabilistic methods were proposed to determine the maximum magnitudes from earthquake catalogs. Probabilistic methods are based on either parametric or non-parametric statistical analyses of seismicity (ROBSON and WHITLOCK 1964; COOKE 1979; PISARENKO *et al.* 1996; KIJKO and GRAHAM 1998; KIJKO and SINGH 2011). The probabilistic approaches may yield different estimates depending on the properties of event catalogs such as the completeness of catalogs and the number of composing events. Representative probabilistic methods are introduced in this study.

The parametric approach is applicable to the event catalog that satisfies the Gutenberg–Richter frequency–magnitude relationship. The set of magnitudes satisfies the probability density function, $f(M)$, which can be written as

$$\begin{aligned} f(M) &= \frac{\beta \exp[-\beta(M - M_{\text{min}})]}{\int_{M_{\text{min}}}^{M_{\text{max}}} \beta \exp[-\beta(m - M_{\text{min}})] dm} \\ &= \frac{\beta \exp[-\beta(M - M_{\text{min}})]}{1 - \exp[-\beta(M_{\text{max}} - M_{\text{min}})]}. \end{aligned} \quad (16)$$

Also, the cumulative distribution function, $F(M)$, is given by

$$F(M) = \int_{M_{\text{min}}}^M f(m) dm = \frac{1 - \exp[-\beta(M - M_{\text{min}})]}{1 - \exp[-\beta(M_{\text{max}} - M_{\text{min}})]}. \quad (17)$$

The maximum magnitude based on the Tate–Pisarenko method is given by (Appendix 1)

$$M_{\text{max}} = M_n + \left(\frac{1}{n}\right) \times \frac{1 - \exp[-\beta(M_{\text{max}} - M_{\text{min}})]}{\beta \exp[-\beta(M_{\text{max}} - M_{\text{min}})]}. \quad (18)$$

A grid-searching algorithm is applied to determine the maximum magnitudes with the Tate–Pisarenko approach.

The Tate–Pisarenko method is applicable to earthquake catalogs that satisfy the Gutenberg–Richter frequency–magnitude relationship. Large-magnitude earthquakes with long recurrence intervals can be included in short-term earthquake catalogs in which the expected upper-bound magnitudes ($M_{\text{max}}^{\text{exp}}$) are much smaller than the observed maximum magnitudes ($M_{\text{max}}^{\text{obs}}$) (Fig. 6). Earthquake catalogs including exceptionally large events often yield unstable M_{max} estimates with the Tate–Pisarenko method. A reasonable M_{max} estimate may be achieved when an appropriate number of events (n in Eq. (18)) is considered (Fig. 6). This procedure is applicable to incomplete catalogs in which minimum magnitudes are not determined correctly. There is the possibility that earthquakes of any magnitude can be missed in historical earthquake catalogs. In this case, the Gutenberg–Richter frequency–magnitude relationship for instrumental earthquake catalogs can be applied.

The maximum magnitude based on non-parametric analysis with order statistics is given by (KIJKO and SINGH 2011; Appendix 1)

$$M_{\text{max}} = 2M_n - (1 - e^{-1}) \sum_{i=0}^{n-1} (e^{-i} M_{n-i}). \quad (19)$$

The Robson–Whitlock (RW) method for M_{max} uses the largest two magnitudes in the catalog (ROBSON and WHITLOCK 1964). The maximum magnitude is determined to be

$$M_{\text{max}} = (n + 1)M_n - nM'_{n-1} = 2M_n - M_{n-1}. \quad (20)$$

The Robson–Whitlock–Cooke (RWC) method for M_{max} is modified from the RW method, which is given by (COOKE 1979; KIJKO and SINGH 2011)

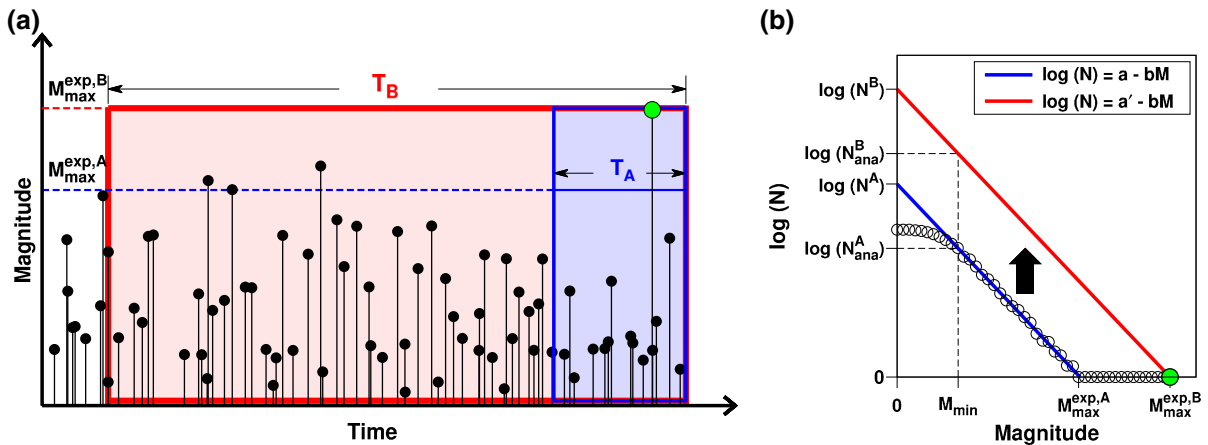


Figure 6

a Distribution of event magnitudes as a function of time in short-period (T_A) and long-period (T_B) catalogs. The expected maximum magnitudes for short and long periods are $M_{\max}^{\text{exp},A}$ and $M_{\max}^{\text{exp},B}$. An excessively large earthquake with magnitude of $M_{\max}^{\text{obs},A}$, satisfying $M_{\max}^{\text{obs},A} = M_{\max}^{\text{exp},B}$, is included in the short-period catalog. **b** The Gutenberg–Richter frequency–magnitude relationships for short-period and long-period catalogs. The numbers of events with magnitudes $M \geq M_{\min}$ for short- and long-period catalogs are N_{ana}^A and N_{ana}^B . The maximum magnitude for the long period is determined using the b value of the short-period catalog

$$M_{\max} = M_n + v(M_n - M_{n-1}), \quad (21)$$

where v is a constant.

These methods have been applied widely to estimate maximum magnitudes in a number of regions including both active and stable regions (e.g., KIJKO 2004; KIJKO and Singh 2011; ANBAZHAGAN *et al.* 2015). The four methods are used to determine the maximum magnitudes of events in the Korean Peninsula based on instrumental and historical earthquake catalogs.

5. Procedure

5.1. Construction of a Seismicity Density Map

The seismicity density map is constructed by combining the epicenters of earthquakes with magnitudes greater than or equal to the minimum magnitudes. The minimum magnitudes of instrumental and historical earthquake records are determined to be M_L 2.5 and 4.7, respectively (Fig. 7). The seismicity density represents the population of seismic events, suggesting earthquake occurrence frequencies. The Korean Peninsula is discretized into 0.1° -by- 0.1° cells. A Gaussian function is applied for spatial smoothing of earthquake occurrence

frequencies. Spatial smoothing enables us to accommodate events with low-precision location information (HOUNG and HONG 2013). The correlation distance of the Gaussian function is set to 20 km, which is sufficiently large considering the hypocenter precision. The seismicity density is calculated by assessing the smoothed number of events.

5.2. Determination of Seismotectonic Provinces and Seismicity Parameters

The damage related to large events was well documented in the historical literature. Historical earthquakes are useful for assessment of long-term seismicity, which should be considered in the construction of seismotectonic provinces. The occurrence of earthquakes is related to both the tectonics and geological features. It is necessary to implement complete earthquake catalogs for correct determination of seismicity properties. The minimum magnitudes ensuring the completeness of earthquake catalogs vary with the spatial coverage of stations, which is dependent on the physical environment. The minimum magnitudes of the offshore regions are inherently higher than those of inland regions.

The seismotectonics characterizes the interaction between seismicity and tectonics by consolidating the

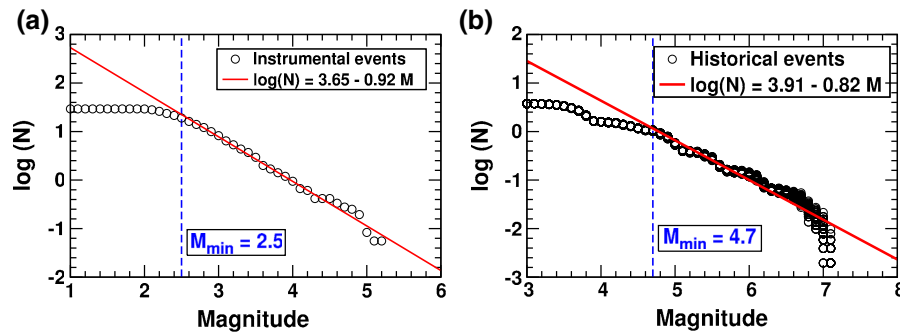


Figure 7

Minimum magnitudes (M_{\min}) ensuring the completeness of earthquake catalogs: **a** instrumental earthquake catalog and **b** historical earthquake catalog. The minimum magnitudes of the instrumental and historical earthquakes are determined to be 2.5 and 4.7, respectively

seismic, geological, geophysical and geodetic properties in the context of a tectonic framework (SCHOLZ 2002). The seismotectonic provinces are regionalized such that each province has unique seismicity and tectonics properties. The seismicity properties and seismic hazards are controlled by various factors including the medium properties and stress field. The medium properties can be inferred from the seismic, geophysical and geological features. Thus, the differences in the seismic, geophysical and geological features suggest different seismotectonic environments. The boundaries of seismotectonic provinces are constructed considering the spatial distribution of geophysical, geological and seismic properties.

We firstly divide the regions based on the seismicity density adequately. Uniform seismicity regions are adjusted considering the spatial distribution of focal mechanisms and geophysical signatures. The seismotectonic province boundaries are constructed considering the geological province boundaries, and seismic and geophysical properties. Also, we determine the minimum magnitudes (M_{\min}) and the Gutenberg–Richter parameters (a , b) for each province. The earthquake frequency parameter, a value, is normalized for time (year) and area (1 km^2). The estimates of maximum magnitudes are generally dependent on the observed maximum magnitudes and the completeness of the catalogs.

The minimum magnitude may vary by the b value, which is dependent on the method implemented. The maximum likelihood method considers every earthquake to be an independent event satisfying the Gutenberg–Richter frequency–magnitude

relationship (AKI 1965; TINTI and MULARGIA 1985). However, the b values for catalogs composed small numbers of events may not be determined accurately using a maximum likelihood method that assigns high weights to small earthquakes and low weights to large earthquakes (WIEMER and WYSS 2000). For better fit of both small and large events, a least-squares method is applied in this study. The range of magnitudes yielding fitnesses less than the threshold level is constrained. We set a magnitude allowing stable estimation of the Gutenberg–Richter relationship to be the minimum magnitude (HOUNG and HONG 2013). Also, we apply four different methods to determine the maximum magnitudes. All analyses are based on the magnitudes in the local magnitude scale (M_L).

6. Synthetic Test of Maximum Magnitude Estimation

We test the validity and limitations of methods for estimation of maximum magnitudes using synthetic data. We produce synthetic earthquake catalogs composed of 100, 200, 500, 1000, 2000, 5000, and 10,000 events. The synthetic earthquake catalogs have a M_{\min} of 2.5 and a b value of 0.92 for tests of instrumental earthquake records, and have a M_{\min} of 4.7 and a b value of 0.82 for tests of historical earthquake records. The maximum magnitude (M_{\max}) is set to 7.5. We generate 1000 different sets of event catalogs to assess the variation in M_{\max} estimates depending on the event catalog. Four methods including the Tate–Pisarenko (TP) method, non-parametric determination based on order statistics

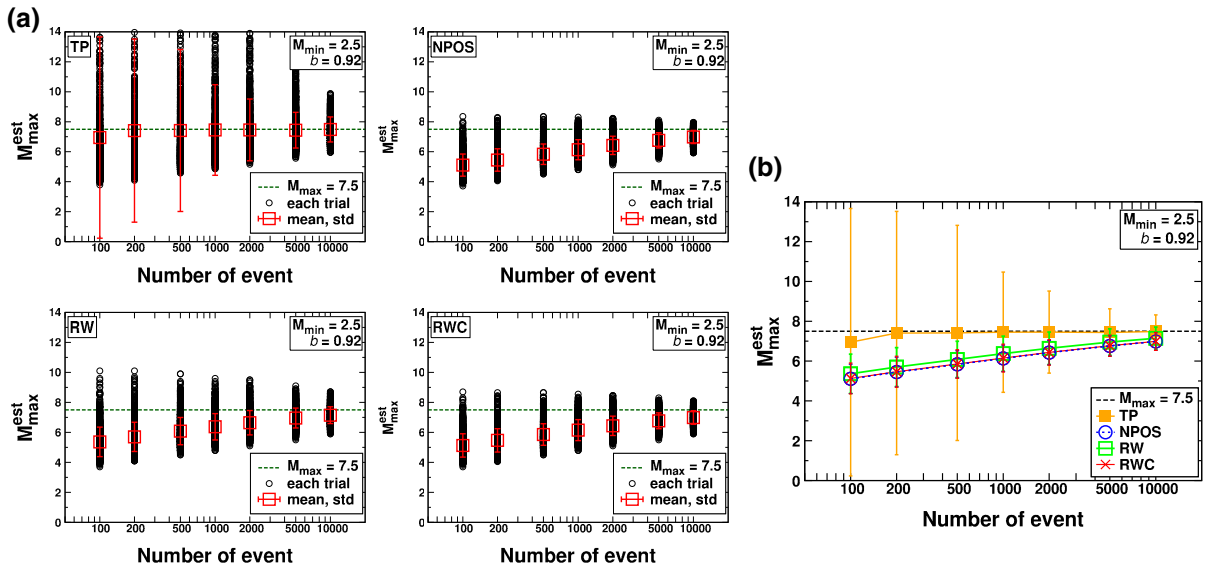


Figure 8

Synthetic tests of maximum magnitude estimation for synthetic earthquake catalogs with the minimum magnitude of 2.5 and b value of 0.92. **a** Variations of maximum magnitude estimates for synthetic earthquake catalogs with various numbers of events. The maximum magnitudes are determined by four methods (TP, NPOS, RW, RWC). The accuracy of estimated maximum magnitudes increases with the number of events in the catalogs. **b** Comparison of maximum magnitude estimates among four methods. Method TP yields the most accurate estimates with large standard deviations

(NPOS), Robson–Whitlock (RW) method, and Robson–Whitlock–Cooke (RWC) method are applied to estimate the maximum magnitudes.

It is observed that maximum magnitude estimates generally approach to the correct maximum magnitude with an increasing number of events in the catalogs (Figs. 8, 9). Also, the standard deviations of the maximum magnitude estimates decrease with the number of events. The parametric method (TP) produces more accurate M_{\max} estimates than non-parametric methods (NPOS, RW, RWC). Also, the Robson–Whitlock (RW) method is the most accurate of the non-parametric methods.

The standard deviations of M_{\max} estimates from the parametric method are greater than those from the non-parametric methods. This observation suggests that M_{\max} estimates are unstable when the event catalog is composed of a small number of events. On the other hand, the non-parametric methods display relatively stable M_{\max} estimates with catalogs with small numbers of events. However, non-parametric methods generally underestimate the maximum magnitudes for catalogs composed of small numbers of events.

It is intriguing to note that the convergence of M_{\max} estimates to the correct value is dependent on the implemented M_{\min} as well as the number of events in the catalog (Figs. 8, 9). A larger number of events in the catalog appears to be needed for correct estimation when a smaller M_{\min} is applied. This is because small events are naturally more frequent than large events according to the Gutenberg–Richter frequency–magnitude relationship.

7. Seismicity Density

The seismicity density models are calculated based on instrumental and historical earthquake records (Fig. 10). Long-term seismicity is represented by historical earthquakes. The historical seismicity density model is observed to be similar to the instrumental seismicity density model in most inland regions. High seismicity densities are found in the Okcheon belt (region A in 10), Taebaeksan basin (region B), Pyeongan basin (region C), and Yeongnam massif (region D) in both the instrumental and historical seismic densities. Low seismicity is

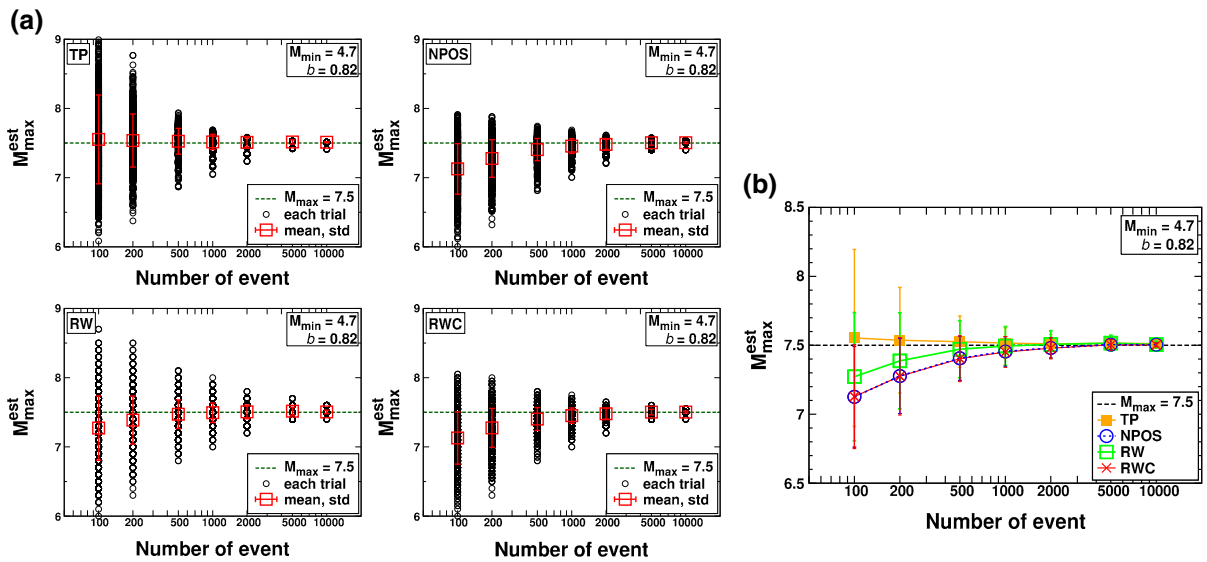


Figure 9

Synthetic tests of maximum magnitude estimation for synthetic earthquake catalogs with the minimum magnitude of 4.7 and b value of 0.82. **a** Variations of maximum magnitude estimates for synthetic earthquake catalogs with various numbers of events. The maximum magnitudes are determined by four methods (TP, NPOS, RW, RWC). **b** Comparison of maximum magnitude estimates among four methods

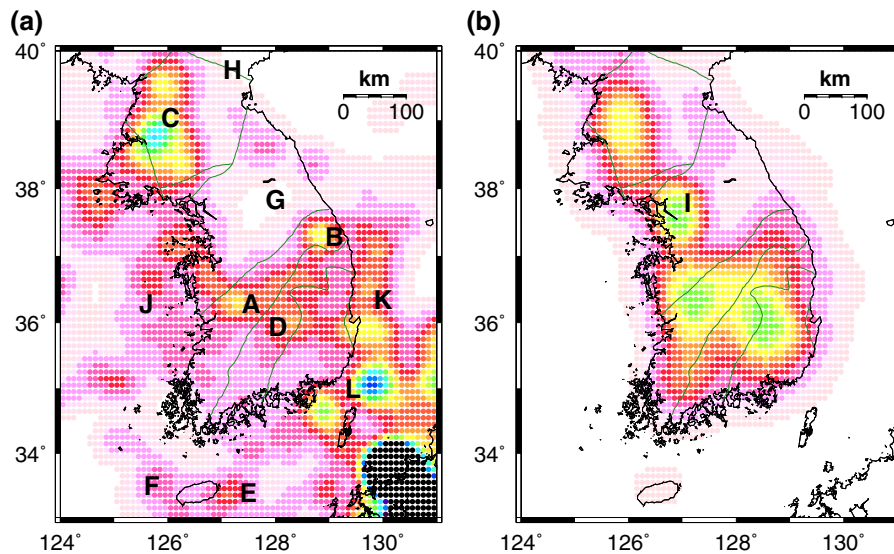


Figure 10

The spatial distribution of seismicity densities based on **a** the instrumental earthquakes with magnitudes greater than or equal to 2.5, and **b** the historical earthquakes with magnitudes greater than or equal to 4.7. High seismicity is observed at similar inland regions between the instrumental and historical catalogs (regions A, B, C, D). Low seismicity is observed in the northeastern peninsula (region H) and Gyeonggi massif (region G). The historical earthquakes display a characteristic high seismicity around the Seoul metropolitan area (region I), and weak seismicity in offshore regions (regions E, F, J, K, L)

observed at the Gyeonggi massif (region G) and northeastern peninsula (region H) in both seismic densities.

We find differences between the historical and instrumental seismicity density models in several regions including the Seoul metropolitan area in the

central peninsula (region I) and offshore regions in the Yellow Sea, East Sea, and South Sea (regions E, F, J, K, L). Historical earthquakes suggest high seismicity densities in the Seoul metropolitan region, while instrumental earthquakes display low seismicity densities. This observation suggests that large events in the Seoul metropolitan region may have long recurrence time intervals. The apparent differences in offshore seismicity between the instrumental and historical earthquake records may be associated with the limited observation of offshore events without help of modern seismic instruments due to physical inaccessibility.

8. Seismotectonic Provinces

Seismotectonic province models are constructed for the region of latitudes between 33° and 40° and longitudes between 124° and 131° . We first consider a seismotectonic province model composed of 17

provinces (Fig. 11). Province 2 is constructed for the highest seismicity region in the northwestern peninsula (Pyeongnam massif). This high seismicity is clearly observed in both the instrumental and historical seismicities. Province 1 is located to the west of province 2. Province 3 is an inland region located to the east of province 2.

Province 4 is an offshore region to the east of province 3. Both provinces 3 and 4 are low seismicity regions. Province 3 includes the eastern Pyeongnam and eastern Gyeonggi massifs. Provinces 3 and 4 are divided considering the physical environment and crustal thickness. Note that the crustal thickness changes abruptly across the east coast of the peninsula. Province 5 includes the region around Baekyeong island and Ongjin basin, which is adjacent to provinces 1 and 2. Province 5 is a high seismicity offshore region. The dominant focal mechanism in the province is normal faulting. Provinces 1 and 5 are divided considering the geological provinces and faulting systems. It was reported that

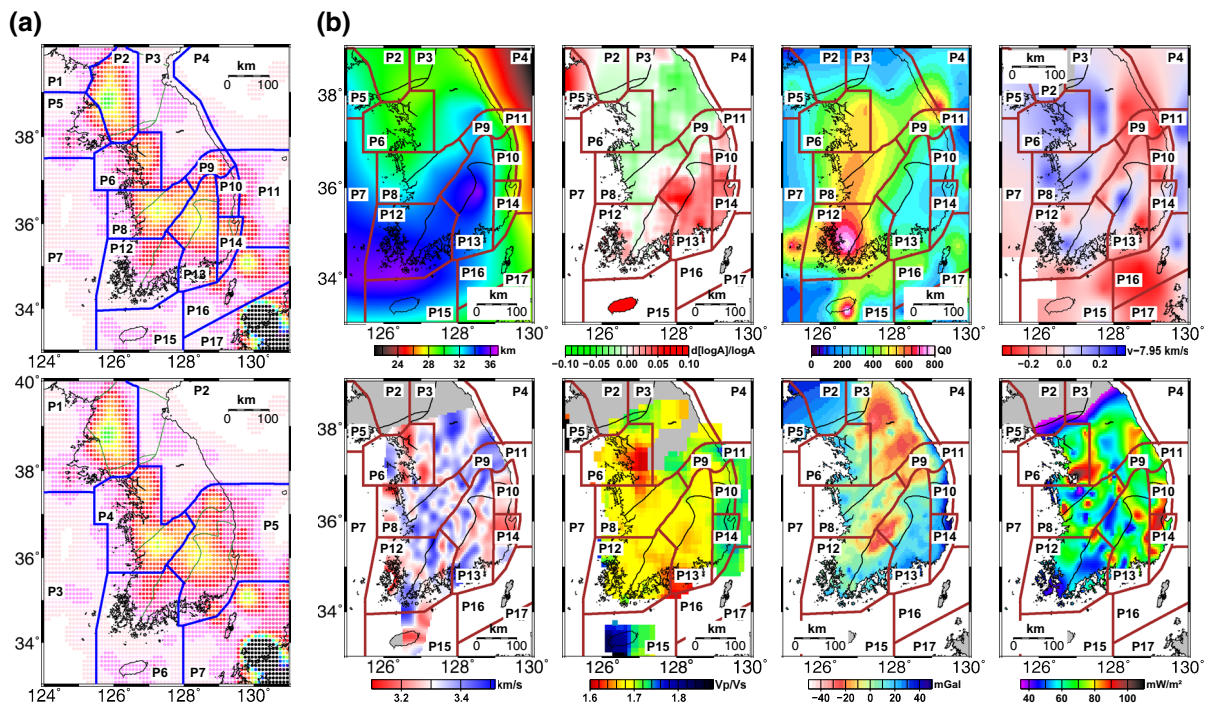


Figure 11

a Seismotectonic province models composed of 17 and 7 provinces over the reference seismicity density map. The 7-province-composite model is a simplified model of the 17-province-composite model. **b** The 17-province-composite model over seismic and geophysical properties. The seismotectonic province model generally agrees with the regional variation of seismic and geophysical properties

the paleo-collision belt between the North and South China blocks may be placed in province 5 (HONG and CHOI 2012).

Province 6 includes the western Gyeonggi massif, which is placed to the west of province 3 and to the south of province 2. Province 6 represents the high historical seismicity region around the Seoul metropolitan area in the central peninsula. Localized high heat flows and low Moho P (Pn) velocities are observed in the region. This province displays a characteristic seismicity with long recurrence time intervals (high historical seismicity but low instrumental seismicity). Province 7 includes the central and southern Yellow Sea regions, which display low and diffuse seismicity. Province 8 is a region including the southern Gyeonggi massif and central Okcheon belt displaying high seismicity in both the instrumental and historical earthquake records. This province displays low heat flows and high Pn velocities. Province 9 represents a localized high seismicity region in the eastern Okcheon belt (Taebaeksan basin). Low Pn velocities and high shallow-crustal S velocities are observed in the region.

Province 10 covers the eastern Yeongnam massif and northeastern Gyeongsang basin, presenting low Pn velocities. Province 11 is the the East Sea region to the south of province 4. This province includes the NS-directional paleo-continental-rifting structure that produces reverse-faulting earthquakes by the ambient compressional stress (CHOI *et al.* 2012). High Pn velocities, localized high Lg Q , and high Bouguer gravity anomalies are observed along the paleo-rifting structure. A transitional structure between the continental and oceanic crusts develops in the region. Province 12 includes the southwestern peninsula of mild seismicity. This province includes the southwestern Okcheon belt and southern Yeongnam massif that are characterized by low heat flows, high Pn velocities, high Lg Q , and high Bouguer gravity anomalies.

Province 13 is located in the south-central peninsula, which includes the central Yeongnam massif and the western Gyeongsang basin. The province is a high seismicity region with low V_P/V_S ratios, low heat flows, high Pn, and high P amplification. Province 14 represents the southeastern Gyeongsang basin, which is characterized by high

V_P/V_S ratios, low shallow-crustal S velocities, high Pn velocities, and low Lg Q . Province 15 is assigned for the western South Sea region including Jeju island where strong instrumental seismicity is observed. Province 16 includes the eastern South Sea region including Tsushima island. Province 17 is the region around the southern Japanese mainland.

We also construct a simplified model composed of 7 provinces by merging the provinces of the 17-province-composite model (Fig. 11). Provinces 1, 2 and 5 in the 17-province-composite model are combined into province 1 in the 7-province-composite model. Provinces 3 and 4 in the 17-province-composite model are assembled into province 2 in the 7-province-composite model. Provinces 6 and 8 in the 17-province-composite model are merged into province 4 in the 7-province-composite model. Provinces 9, 10, 11, 13 and 14 in the 17-province-composite model comprise province 5 in the 7-province-composite model. Provinces 12 and 15 in the 17-province-composite model comprise province 6 in the 7-province-composite model. Also, provinces 16 and 17 in the 17-province-composite model are combined into province 7 in the 7-province-composite model.

9. Seismicity Properties and Maximum Magnitudes

The Gutenberg–Richter a values for instrumental earthquake catalogs are observed to be larger than those for historical earthquake catalogs. This may be because the historical earthquake catalog is not complete. Note that inhomogeneous distribution of major towns and cities causes location-dependent records of historical earthquakes (HOUNG and HONG 2013). The b values for instrumental earthquakes vary between 0.54 and 1.25 in the 7-province-composite model, and between 0.31 and 1.45 in the 17-province-composite model. The b values for the historical earthquakes are 0.55–0.91 in the 7-province-composite model and 0.34–0.85 in the 17-province-composite model. It is noteworthy that the b values of the 7-province-composite model are close to those of the 17-province-composite model for the same regions. The b values for the instrumental earthquakes are applied in the determination of maximum magnitudes of historical earthquakes

considering possible incomplete historical earthquake records.

The expected maximum magnitudes (M_{\max}^{exp}) are calculated with estimated a and b values for the duration of the earthquake catalogs, and are compared with the observed maximum magnitudes (M_{\max}^{obs}). The differences between M_{\max}^{obs} and M_{\max}^{exp} for instrumental earthquake catalogs are less than 0.5 magnitude unit in most regions except province 7 of the 7-province-composite model and province 17 of the 17-province-composite model where the differences are found to be 1.10 and 1.11. The large differences suggest possible unstable estimation of M_{\max} with a parametric method (TP method).

The maximum magnitudes are estimated using four different methods (TP, NPOS, RW, RWC). In addition, the maximum magnitudes for T_{exp} are estimated using the TP method. The maximum magnitude estimates of the instrumental earthquakes are 4.90–7.50 (TP*), 4.62–7.51 (NPOS), 4.80–8.20 (RW), and 4.65–7.60 (RWC) for the 7-province-composite model, and 3.75–7.51 (TP*), 3.51–7.51 (NPOS), 3.60–8.20 (RW), and 3.50–7.60 (RWC) for the 17-province-composite model (Fig. 12). The interval between the upper and lower bounds of the maximum magnitude estimates for the seismotectonic

province model generally increases with the number of constituent provinces. This observation suggests that we may need an appropriate number of constituent provinces for reasonable estimation of maximum magnitudes.

Analysis based on the instrumental earthquake catalog suggests that province 2 of the 17-province-composite model has relatively low estimated maximum magnitudes despite characteristic high seismicity with a large b value. This may be because the observed maximum magnitude of province 2 is lower than those of other provinces (Table 2). Also, characteristic regional variation in maximum magnitude estimates is observed in the 17-province-composite model where province 10, a low seismicity region surrounded by high-seismicity neighbors, displays noticeably low maximum magnitude estimates.

The maximum magnitudes of the historical earthquake catalog are found to be ~ 2.0 magnitude units greater than those of the instrumental earthquake catalog for both the 7- and 17-province-composite models. Maximum magnitudes are not estimated for provinces 3 and 7 in the 7-province-composite model and provinces 4, 15, 16 and 17 in the 17-province-composite model in which historical

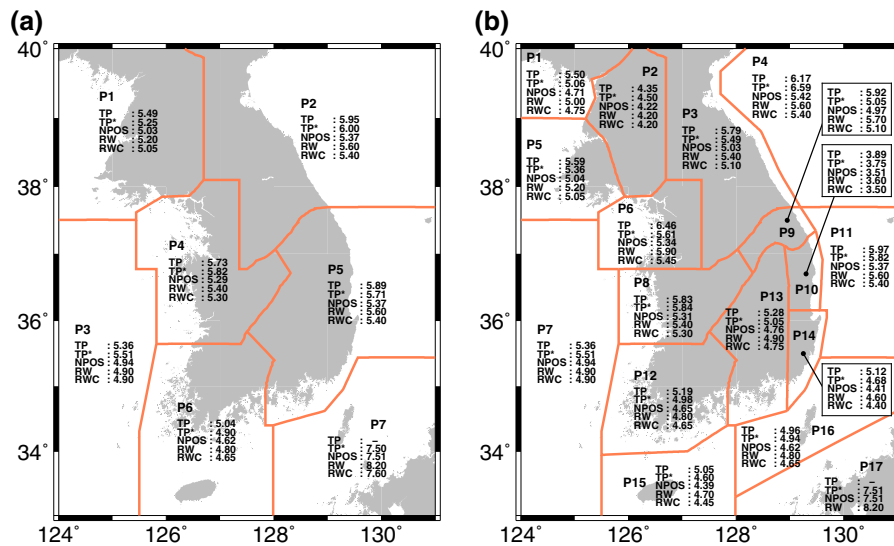


Figure 12

Maximum magnitude estimates based on the instrumental earthquake records for **a** the 7-province-composite seismotectonic province model and **b** the 17-province-composite seismotectonic province model

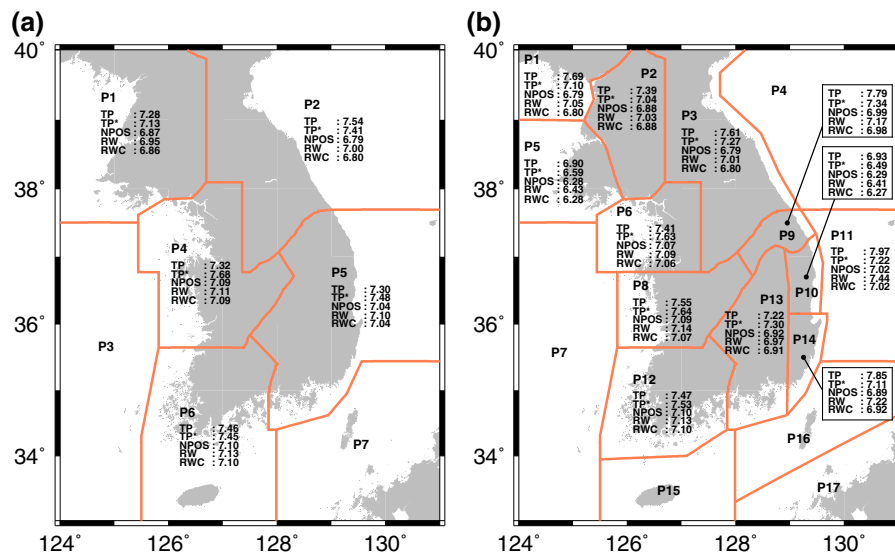


Figure 13

Maximum magnitude estimates based on the historical earthquake records for **a** the 7-province-composite seismotectonic province model and **b** the 17-province-composite seismotectonic province model

earthquake records are limitedly available. The maximum magnitude estimates are found to be 7.13–7.68 (TP*), 6.79–7.10 (NPOS), 6.95–7.13 (RW), and 6.80–7.10 (RWC) for the 7-province-composite model, and 6.49–7.64 (TP*), 6.29–7.10 (NPOS), 6.41–7.44 (RW), and 6.27–7.10 (RWC) for the 17-province-composite model (Fig. 13). The maximum magnitudes of most provinces in the 7-province-composite model are comparable. The distribution of maximum magnitudes suggests a high possibility of large events with magnitudes greater than 7.0 around the peninsula.

The parametric method (the TP method) produces larger maximum magnitude estimates than the non-parametric methods for both instrumental and historical earthquake catalogs. The RW method yields slightly larger estimates than the other non-parametric methods (NPOS, RWC). The NPOS and RWC methods produce comparable maximum magnitudes. These observations are consistent with the synthetic tests (Figs. 8, 9). However, the synthetic experiments suggest that the maximum magnitudes can be under- or over-estimated depending on the number of events in the catalogs (Figs. 8, 9). Also, the error size is dependent on the method and true maximum magnitude. Thus, it may be useful to compare the maximum magnitude

estimates from the four methods to identify possible under- or over-estimation.

Maximum magnitude estimates based on the historical earthquake catalog are greater than those based on the instrumental earthquake catalog due to differences in the observed maximum magnitudes (M_{\max}^{obs}) (Tables 1, 2, 3, 4). The maximum magnitude estimates based on the historical earthquake catalog appear to be more suitable for assessment of seismic hazard potentials than those based on the instrumental earthquake catalog. There were several studies investigating M_{\max} in the Korean Peninsula (KIM *et al.* 2000; LEE 2001; NOH 2014). KIM *et al.* 2000 presented maximum magnitudes of 6.97–7.45, and LEE (2001) suggested 7.06–7.88 from analysis of historical earthquakes. On the other hand, NOH (2014) suggested the maximum magnitude of events in the Korean Peninsula to be 6.98 from the analysis of instrumental earthquakes. The maximum magnitudes of the previous studies are generally comparable or slightly greater than those seen in this study.

10. Discussion and Conclusions

We analyzed long-period earthquake records combining instrumental and historical earthquake

Table 1

Seismicity properties and maximum magnitude estimates of instrumental earthquakes for the 7-province-composite seismotectonic province model

ID	N_{obs}	M_{max}^{obs}	M_{min}	N_{ana}	\bar{a}	b	ϵ (%)	M_{max}^{exp}	T_{exp} (years)	M_{max}				
										TP	TP*	NPOS	RW	RWC
P1	256	4.9	3.15	90	-0.19	1.25	6.81	4.86	39.91	5.49	5.25	5.03	5.20	5.05
P2	61	5.2	1.95	61	-3.53	0.54	9.11	5.43	27.17	5.95	6.00	5.37	5.60	5.40
P3	100	4.9	2.35	88	-2.54	0.72	8.12	5.28	19.10	5.36	5.51	4.94	4.90	4.90
P4	223	5.2	1.95	222	-2.29	0.70	5.08	5.47	23.31	5.73	5.82	5.29	5.40	5.30
P5	444	5.2	1.95	439	-1.81	0.86	6.88	5.33	28.09	5.89	5.71	5.37	5.60	5.40
P6	149	4.5	2.75	60	-1.35	1.10	6.04	4.49	37.20	5.04	4.90	4.62	4.80	4.65
P7	8767	7.0	1.55	4046	-1.16	0.87	3.56	5.89	329.08	-	7.50	7.51	8.20	7.60

The time duration of data set (T_{obs}) is 36 years

ID: province

N_{obs} , number of observed earthquakes, M_{max}^{obs} , observed maximum magnitude, M_{min} minimum magnitude, N_{ana} number of earthquakes with $M \geq M_{min}$, \bar{a} Gutenberg–Richter earthquake occurrence rate normalized for time (years) and area (km^2), b Gutenberg–Richter frequency–magnitude ratio, ϵ residuals between observed data set and Gutenberg–Richter frequency–magnitude line, M_{max}^{exp} expected maximum magnitude for time period T_{obs} , T_{exp} theoretical recurrence interval for M_{max}^{obs} , M_{max} maximum magnitude estimate, TP Tate–Pisarenko method, TP^* Tate–Pisarenko method based on T_{exp} , $NPOS$ non-parameter determination based on order statistics, RW Robson–Whitlock method, RWC Robson–Whitlock–Cooke method

Table 2

Seismicity properties and maximum magnitude estimates of instrumental earthquakes for the 17-province-composite seismotectonic province model

ID	N_{obs}	M_{max}^{obs}	M_{min}	N_{ana}	\bar{a}	b	ϵ (%)	M_{max}^{exp}	T_{exp} (years)	M_{max}				
										TP	TP*	NPOS	RW	RWC
P1	11	4.5	2.95	9	-2.21	0.78	13.84	4.37	45.76	5.50	5.06	4.71	5.00	4.75
P2	153	4.2	3.35	32	0.63	1.45	3.65	4.45	15.81	4.35	4.50	4.22	4.20	4.20
P3	43	4.8	1.95	43	-3.12	0.63	10.75	4.73	39.71	5.79	5.49	5.03	5.40	5.10
P4	13	5.2	2.05	13	-4.48	0.31	14.44	5.63	26.48	6.17	6.59	5.42	5.60	5.40
P5	92	4.9	2.95	46	-1.23	0.94	6.57	4.89	37.00	5.59	5.36	5.04	5.20	5.05
P6	61	5.0	1.95	61	-2.46	0.71	10.64	4.71	58.00	6.46	5.61	5.34	5.90	5.45
P7	100	4.9	2.35	88	-2.54	0.72	8.12	5.28	19.10	5.36	5.51	4.94	4.90	4.90
P8	167	5.2	1.95	166	-2.23	0.68	5.70	5.31	30.27	5.83	5.84	5.31	5.40	5.30
P9	41	4.5	1.95	41	-2.09	0.80	26.07	4.00	90.23	5.92	5.05	4.97	5.70	5.10
P10	29	3.4	2.15	26	-0.97	1.26	9.12	3.41	35.05	3.89	3.75	3.51	3.60	3.50
P11	152	5.2	1.95	150	-2.19	0.70	8.93	5.41	25.56	5.97	5.82	5.37	5.60	5.40
P12	69	4.5	2.65	33	-1.98	0.91	5.94	4.45	39.90	5.19	4.98	4.65	4.80	4.65
P13	175	4.6	2.15	153	-1.54	0.96	4.08	4.51	44.01	5.28	5.05	4.76	4.90	4.75
P14	47	4.2	2.05	46	-1.71	0.90	8.47	4.02	52.22	5.12	4.68	4.41	4.60	4.40
P15	80	4.2	2.15	78	-1.46	1.08	9.85	4.10	45.79	5.05	4.60	4.39	4.70	4.45
P16	620	4.5	1.85	380	-1.37	0.98	7.73	4.71	22.45	4.96	4.94	4.62	4.80	4.65
P17	8147	7.0	1.45	4213	-0.94	0.85	3.33	5.90	311.04	-	7.51	7.51	8.20	7.60

The time duration of data set (T_{obs}) is 36 years

catalogs for assessment of seismic hazard potentials. Seismotectonic province models were proposed for the Korean Peninsula, which belongs to an intraplate regime with low and diffuse seismicity. The seismotectonic provinces were identified from the

seismicity properties models, and their boundaries were defined considering the geological, geophysical and tectonic properties. Seismotectonic province models that are composed of 7 and 17 provinces were proposed. The maximum magnitudes and seismicity

Table 3

Seismicity properties and maximum magnitude estimates of historical earthquakes for the 7-province-composite seismotectonic province model

ID	N_{obs}	$M_{\text{max}}^{\text{obs}}$	M_{min}	N_{ana}	\bar{a}	b	ϵ (%)	$M_{\text{max}}^{\text{exp}}$	T_{exp} (years)	M_{max}				
										TP	TP ^a	NPOS	RW	RWC
P1	611	6.78	4.20	241	-1.31	0.88	6.30	5.79	9613.59	7.28	7.13	6.87	6.95	6.86
P2	89	6.60	4.06	54	-2.49	0.79	9.20	7.56	171.35	7.54	7.41	6.79	7.00	6.80
P4	625	7.06	4.09	412	-1.41	0.76	4.30	7.11	470.65	7.32	7.68	7.09	7.11	7.09
P5	414	6.97	4.67	173	-0.85	0.91	6.02	6.67	946.74	7.30	7.48	7.04	7.10	7.04
P6	150	7.06	3.63	131	-3.12	0.55	4.66	5.54	23,834.01	7.46	7.45	7.10	7.13	7.10

The time duration of data set (T_{obs}) is 512 years

^a The seismic properties and maximum magnitudes estimated are not provided for provinces 3 and 7 where historical earthquake records were limited

Table 4

Seismicity properties and maximum magnitude estimates of historical earthquakes for the 17-province-composite seismotectonic province model

ID	N_{obs}	$M_{\text{max}}^{\text{obs}}$	M_{min}	N_{ana}	\bar{a}	b	ϵ (%)	$M_{\text{max}}^{\text{exp}}$	T_{exp} (years)	M_{max}				
										TP	TP ^a	NPOS	RW	RWC
P1	24	6.55	3.74	19	-3.53	0.50	11.58	5.84	1921.59	7.69	7.10	6.79	7.05	6.80
P2	536	6.74	3.52	424	-1.27	0.84	7.35	5.24	90647.30	7.39	7.04	6.88	7.03	6.88
P3	81	6.58	3.95	53	-2.28	0.77	10.01	6.57	600.46	7.61	7.27	6.79	7.01	6.80
P5	50	6.13	3.51	44	-2.97	0.63	9.88	6.11	674.83	6.90	6.59	6.28	6.43	6.28
P6	324	7.02	3.62	269	-2.36	0.60	4.95	6.33	1588.78	7.41	7.63	7.07	7.09	7.06
P8	303	7.00	4.16	174	-1.19	0.81	5.88	7.00	518.02	7.55	7.64	7.09	7.14	7.07
P9	31	6.79	4.18	21	-2.56	0.57	10.36	5.45	6361.92	7.79	7.34	6.99	7.17	6.98
P10	27	6.14	3.85	21	-2.65	0.60	9.92	4.33	186396.83	6.93	6.49	6.29	6.41	6.27
P11	11	6.60	3.73	9	-4.93	0.34	20.86	7.06	255.90	7.97	7.22	7.02	7.44	7.02
P12	149	7.06	3.66	129	-2.87	0.55	4.67	5.72	8524.66	7.47	7.53	7.10	7.13	7.10
P13	299	6.85	4.61	125	-0.93	0.85	5.63	5.71	6878.38	7.22	7.30	6.92	6.97	6.91
P14	43	6.63	3.77	34	-2.28	0.65	11.15	5.30	10,518.40	7.85	7.11	6.89	7.22	6.92

The time duration of data set (T_{obs}) is 512 years

^a The seismic properties and maximum magnitudes estimated are not provided for provinces 4, 7, 15, 16 and 17 where historical earthquake records were limited

properties were calculated for the proposed seismotectonic province models. The maximum magnitudes were determined using four methods (TP, NPOS, RW, RWC).

The validity and accuracy of the four methods were tested through synthetic experiments. The synthetic tests indicated that the accuracy of the estimated maximum magnitudes generally increases with the number of events in the catalog. It was observed that the parametric method (TP) yields more accurate maximum magnitude estimates than non-parametric methods (NPOS, RW, RWC). A modified parametric approach (modified Tate–Pisarenko

method) was proposed for reasonable estimation of maximum magnitudes for short-period or incomplete catalogs with large $M_{\text{max}}^{\text{obs}}$. The modified TP method allowed us to determine the maximum magnitudes of potential earthquakes using the Gutenberg–Richter frequency–magnitude relationship.

The synthetic experiments indicated that the standard deviations of maximum magnitude estimates from the parametric method are greater than those from the non-parametric methods. It was suggested that the maximum magnitudes can be under- or over-estimated using earthquake catalogs composed of a small number of events. It appeared that comparisons

of maximum magnitude estimates among the four methods may be useful for identification of correct maximum magnitudes.

It was observed that the upper bound of estimated maximum magnitudes apparently increases with the number of constituent seismotectonic provinces. Also, when one province is divided into several provinces, the maximum magnitude and b value for the original single province are approximately equal to the averages of the maximum magnitudes and b values for the subdivided provinces. These observations suggested that an appropriate number of constituent provinces are needed for correct assessment of seismic hazard potentials. Analysis based on the historical earthquake catalog yielded larger maximum magnitudes than those based on the instrumental earthquake catalog. The maximum magnitudes estimated in this study were generally smaller than those of previous studies. The maximum magnitudes suggested a high possibility of large events with magnitudes greater than 7.0 around the peninsula.

Acknowledgments

We are grateful to the Korea Meteorological Administration (KMA) for making seismic data available. We thank Professor Andrzej Kijko and an anonymous reviewer for their constructive review comments, which improved this manuscript. This work was supported by the Korea Meteorological Administration Research and Development Program under Grant KMIPA 2015-7040.

Appendix 1: Determination of M_{\max}

Parametric Determination: The Tate–Pisarenko (TP) Method

An event catalog composed of n events is considered. The magnitudes of the events are M_j ($j = 1, 2, \dots, n$) in an ascending order. We define the probability, $G(M, Y)$ that $F(M)$ is less than a certain constant Y (PISARENKO *et al.* 1996; KIJKO and GRAHAM 1998):

$$G(M, Y) = \text{Probability}[F(M) \leq Y] = Y, \tag{22}$$

where the constant Y ranges between 0 and 1. The probability for the case that $F(M_n)$ is less than Y is given by

$$G(M_n, Y) = \text{Probability}[F(M_n) \leq Y] = Y^n. \tag{23}$$

The differentiation of $G(M_n, Y)$ with respect to Y corresponds to $F(M_n)$:

$$\frac{dG(M_n, Y)}{dY} = nY^{n-1} = g(M_n, Y). \tag{24}$$

Here, function $g(M_n)$ is given by

$$\begin{aligned} g(M_n, Y) &= \text{Probability}[f(M_n) \leq Y] \\ &= \text{Probability}[f(M_1) \leq Y, \\ &\quad f(M_2) \leq Y, \dots, f(M_n) \leq Y] \\ &= \int f(M) dm \\ &= F(M_n) \end{aligned} \tag{25}$$

The expected value of $F(M_n)$, S_n , is given by

$$S_n = \int_0^1 F(M_n) Y dY = \int_0^1 g(M_n, Y) Y dY = \frac{n}{n+1}. \tag{26}$$

Here, the expected value S_n is used as the representative value of $F(M_n)$.

The magnitude M_n can be written using a Taylor expansion:

$$M_n = F^{-1}(S_n) = F^{-1}(1) + \left. \frac{dF^{-1}(S)}{dS} \right|_{S=1} (S_n - 1) + \dots, \tag{27}$$

where $F^{-1}(1)$ is equal to M_{\max} , and $S_n = F(M_n) = n/(n+1)$. Also, we have

$$\left. \frac{dF^{-1}(S)}{dS} \right|_{S=1} = \frac{1}{\left. \frac{dF(M)}{dM} \right|_{M=F^{-1}(1)}} = \frac{1}{f(M_{\max})}. \tag{28}$$

Thus, Eq. (27) becomes

$$M_n = M_{\max} + \frac{1}{f(M_{\max})} \times \left(\frac{-1}{n+1} \right). \tag{29}$$

From Eqs. (29) and (16), the maximum magnitude (M_{\max}) can be rewritten as

$$M_{\max} = M_n + \left(\frac{1}{n+1}\right) \times \frac{1 - \exp[-\beta(M_{\max} - M_{\min})]}{\beta \exp[-\beta(M_{\max} - M_{\min})]}, \quad (30)$$

which can be approximated for a large n as

$$M_{\max} = M_n + \left(\frac{1}{n}\right) \times \frac{1 - \exp[-\beta(M_{\max} - M_{\min})]}{\beta \exp[-\beta(M_{\max} - M_{\min})]}. \quad (31)$$

Non-Parametric Determination Based on Order Statistics (NPOS)

The expected value of magnitude, $E(M)$, can be calculated using

$$E(M) = \int_{M_{\min}}^{M_{\max}} Mf(M)dM = M_{\max} - \int_{M_{\min}}^{M_{\max}} F(M) dM. \quad (32)$$

The cumulative probability density function, $F(M)$, is given by

$$F(M) = \text{Probability}[M \leq M_u], \quad (33)$$

where M_u is a given magnitude. Equation (33) suggests that

$$F(M_n) = \text{Probability}[M_1 \leq M_u, M_2 \leq M_u, \dots, M_n \leq M_u] = [F(M)]^n. \quad (34)$$

Thus, we have

$$E(M_n) = M_{\max} - \int_{M_{\min}}^{M_{\max}} [F(M)]^n dM. \quad (35)$$

The integration over magnitude up to M_{\max} corresponds to integration over magnitude up to M_n , and the expected value of $E(M_n)$ is replaced to be M_n . We have

$$M_{\max} = M_n + \int_{M_{\min}}^{M_n} [F(M)]^n dM, \quad (36)$$

where the cumulative probability function, $F(M)$, can be written as (COOKE 1979; KUKO and SINGH 2011)

$$F(M) = \frac{i}{n}, \quad \text{for } (1 \leq i \leq n). \quad (37)$$

The expression for M_{\max} in Eq. (36) can be written in a discrete form using Eq. (37):

$$M_{\max} = M_n + \sum_{i=1}^{n-1} \left(\frac{i}{n}\right)^n (M_{i+1} - M_i) = M_n + M_n - \sum_{i=0}^{n-1} \left[\left\{ \left(1 - \frac{i}{n}\right)^n - \left(1 - \frac{i+1}{n}\right)^n \right\} M_{n-i} \right]. \quad (38)$$

From the definition of natural logarithm, we have

$$\lim_{n \rightarrow \infty} \left(1 + \frac{1}{n}\right)^n = e. \quad (39)$$

Equation (38) becomes

$$M_{\max} = 2M_n - (1 - e^{-1}) \sum_{i=0}^{n-1} (e^{-i} M_{n-i}). \quad (40)$$

The Robson–Whitlock (RW) Method

This method uses the largest two magnitudes in the catalog (ROBSON and WHITLOCK 1964). From Eq. (29), we deduce a relationship for an event catalog that is composed of $n - 1$ events:

$$M'_{n-1} = M_{\max} + \frac{1}{f(M_{\max})} \times \left(\frac{-1}{n}\right). \quad (41)$$

Here, when we select $n - 1$ events from n events, the average of the observed maximum magnitudes in the selected catalogs:

$$M'_{n-1} = \frac{(n - 1)M_n + M_{n-1}}{n}. \quad (42)$$

Thus, from Eqs. (29), (41) and (42), we have

$$M_{\max} = (n + 1)M_n - nM'_{n-1} = 2M_n - M_{n-1}. \quad (43)$$

REFERENCES

AKI, K. (1965). Maximum likelihood estimate of b in the formula $\log N = a - bM$ and its confidence limits, Bulletin of the Earthquake Research Institute, University of Tokyo 43, 237-239.
 AKI, K., and P.G. RICHARDS (2002). Quantitative Seismology, 2nd ed., University Science Books, Sausalito, CA.
 ANBAZHAGAN, P., K. BAJAJ, S. S. MOUSTAFA, and N. S. AL-ARIFI (2015). Maximum magnitude estimation considering the regional rupture character, Journal of Seismology, 19(3), 695-719.
 ARAI, H., and K. TOKIMATSU (2004). S-wave velocity profiling by inversion of microtremor H/V spectrum, Bulletin of the Seismological Society of America, 94, 53-63.

- BENDER, B. (1983). *Maximum likelihood estimation of b values for magnitude grouped data*, Bulletin of the Seismological Society of America, 73, 831-851.
- CHO, H.-M., H.-J. KIM, H.-T. JOU, J.-K. HONG, and C.-E. BAAG (2004). *Transition from rifted continental to oceanic crust at the southeastern Korean margin in the East Sea (Japan Sea)*, Geophysical Research Letters, 31, L07606, doi:10.1029/2003GL019107.
- CHOI, H., T.-K. HONG, X. HE, and C.-E. BAAG (2012). *Seismic evidence for reverse activation of a paleo-rifting system in the East Sea (Sea of Japan)*, Tectonophysics, 572-573, 123-133.
- CHOI, J., T.-S. KANG, C.-E. BAAG (2009). *Three-dimensional surface wave tomography for the upper crustal velocity structure of southern Korea using seismic noise correlations*, Geosciences Journal, 13 (4), 423-432.
- CHOI, S.J. (2012). *Active Fault Map and Seismic Hazard Map*, Research Report, NEMA-Jayeon-2009-24, National Emergency Management Agency, p.953. (in Korean)
- CHOUGH, S.K., S.-T. KWON, J.-H. REE, and D.-K. CHOI (2000). *Tectonic and sedimentary evolution of the Korean Peninsula: a review and new view*, Earth-Science Reviews, 52, 175-235.
- COOKE, P. (1979). *Statistical inference for bounds of random variables*, Biometrika 66, 367-374.
- CORNELL, C. (1968). *Engineering seismic risk analysis*, Bulletin of the Seismological Society of America, 58, 1583-1606.
- COSTA, G., I. OROZOVA-STANISHKOVA, G.F. PANZA, and I.M. ROTWAIN (1996). *Seismotectonic models and CN algorithm: The case of Italy*, Pure and Applied Geophysics, 147 (1), 119-130.
- CUI, P., X. Q. CHEN, Y. Y. ZHU, F. H. SU, F. Q. WEI, Y. S. HAN, G. J. LIU, and J. Q. ZHUANG (2011). *The Wenchuan earthquake (May 12, 2008), Sichuan province, China, and resulting geohazards*, Natural Hazards 56, 19-36.
- DE, R. and J.R. KAYAL (2003). *Seismotectonic model of the Sikkim Himalaya: constraint from microearthquake surveys*, Bulletin of the Seismological Society of America, 93 (3), 1395-1400.
- ENGD AHL, E. R., and A. VILLASENOR (2002). *Global Seismicity: 1900-1999*, in International Handbook of Earthquake and Engineering Seismology, Part A, W. H. K. Lee, H. Kanamori, P. C. Jennings, and C. Kisslinger (Editors), Chapter 41, Academic Press, New York, 665-690.
- FRANKEL, A. (1995). *Mapping seismic hazard in the central and eastern United States*, Seismological Research Letters, 66 (4), 8-21.
- GASPARINI, C., G. IANACCONE, P. SCANDONE, and R. SCARPA (1982). *Seismotectonics of the Calabrian arc*, Tectonophysics, 84 (2-4), 267-286.
- GOMBERG, J. (1991). *Seismicity and detection/location threshold in the southern Great Basin seismic network*, Journal of Geophysical Research 96, 16,401-16,414.
- HE, X. and T.-K. HONG (2010). *Evidence for strong ground motion by waves refracted from the Conrad discontinuity*, Bulletin of the Seismological Society of America, 100 (3), 1370-1374.
- HIRATA, N., B.Y. KARP, T. YAMAGUCHI, T. KANAZAWA, K. SUYEHRO, J. KASAHARA, H. SHIOBARA, M. SHINOHARA, and H. KINOSHITA (1992). *Oceanic crust in the Japan Basin of the Japan Sea by the 1990 Japan-USSR expedition*, Geophysical Research Letters, 19, 2027-2030.
- HONG, T.-K. (2010). *Lg attenuation in a region with both continental and oceanic environments*, Bulletin of the Seismological Society of America, 100 (2), 851-858.
- HONG, T.-K., C.-E. BAAG, H. CHOI, and D.-H. SHEEN (2008). *Regional seismic observations of the 9 October 2006 underground nuclear explosion in North Korea and the influence of crustal structure on regional phases*, Journal of Geophysical Research, 113, B03305, doi:10.1029/2007JB004950.
- HONG, T.-K., and H. CHOI (2012). *Seismological constraints on the collision belt between the North and South China blocks in the Yellow Sea*, Tectonophysics, 570-571, 102-113.
- HONG, T.-K. and KANG, T.-S. (2009). *Pn travel-time tomography of the paleo-continental-collision and rifting zone around Korea and Japan*, Bulletin of the Seismological Society of America, 99 (1), 416-421.
- HONG, T.-K., and K. LEE (2012). *mb(Pn) scale for the Korean Peninsula and site-dependent Pn amplification*, Pure and Applied Geophysics, 169 (11), 1963-1975.
- HONG, T.-K., J. LEE, and S.E. HOUNG (2015). *Long-term evolution of intraplate seismicity in stress shadows after a megathrust*, Physics of the Earth and Planetary Interiors, 245, 59-70.
- HOUNG, S.-E., and T.-K. HONG (2013). *Probabilistic analysis of the Korean historical earthquake records*, Bulletin of the Seismological Society of America, 103 (5), 2782-2796.
- JO, E., and T.-K. HONG (2013). *Vp/Vs ratios in the upper crust of the southern Korean Peninsula and their correlations with seismic and geophysical properties*, Journal of Asian Earth Sciences, 66, 204-214.
- JOLIVET, L., K. TAMAKI, and M. FOURNIER (1994). *Japan Sea, opening history and mechanism: A synthesis*, Journal of Geophysical Research, 99, 22,237-22,259.
- KUKO, A. (2004). *Estimation of the maximum earthquake magnitude, m_{max}* , Pure and Applied Geophysics, 161(8), 1655-1681.
- KUKO, A., and G. GRAHAM (1998). *Parametric-historic procedure for probabilistic seismic hazard analysis. Part I: Estimation of maximum regional magnitude m_{max}* , Pure and Applied Geophysics, 152, 413-442.
- KUKO, A., and M. SINGH (2011). *Statistical tools for maximum possible earthquake magnitude estimation*, Acta Geophysica, 59, 674-700.
- KIM, H.-J., S.-J. HAN, G.H. LEE, and S. HUH (1998). *Seismic study of the Ulleung Basin crust and its implications for the opening of the East Sea (Japan Sea)*, Marine Geophysical Research, 20, 219-237.
- KIM, S.G., and S.K. LEE (2000). *Seismic risk map of Korea obtained by using South and North Korea earthquake catalogues*, Journal of the Earthquake Engineering Society of Korea, 4 (1), 13-34, (in Korean).
- KIM, S.K., J. M. LEE, and J. K. KIM (2000). *On the maximum probable earthquakes in the Korean Peninsula*, Proceeding of Spring Conference, Earthquake Engineering Society of Korea, pp. 21-27.
- KYUNG, J.B. (2003). *Paleoseismology of the Yangsan fault, south-eastern part of the Korea peninsula*, Annals of Geophysics, 46, 983-996.
- LAVECCHIA, G.L., F. BROZZETTI, M. BARCHI, M. MENICETTI, and J.V.A. KELLER (1994). *Seismotectonic zoning in east-central Italy deduced from an analysis of the Neogene to present deformations and related stress fields*, 106, 1107-1120.
- LEE, H.K., and J.S. YANG (2007). *ESR dating of the Eupchon fault, South Korea*, Quaternary Geochronology, 2, 392-397.
- LEE, K. (1998). *Historical earthquake data of Korea*, Journal of Korea Geophysical Society, 1, 3-22 (in Korean).

- LEE, K. (2001). Maximum earthquakes in the Korean Peninsula, Proceeding of Spring Conference, Earthquake Engineering Society of Korea, pp. 41-50.
- LEE, K., and W.-S. YANG (2006). *Historical seismicity of Korea*, Bulletin of the Seismological Society of America, 96, 846-855.
- LEE, K., and R.Y. UM (1992). *Geoelectric survey of the Ulsan fault; Geophysical studies on major faults in the Kyeongsan Basins*, Journal of Geological Society of Korea, 28, 32-39.
- LEE, Y.M., S. PARK, J. KIM, H.C. KIM, M.-H. KOO (2010). *Geothermal resource assessment in Korea*, Renewable and Sustainable Energy Reviews 14, 2392-2400.
- MARZOCCHI, W., and L. SANDRI (2003). *A review and new insights on the estimation of the b-value and its uncertainty*, Annals of Geophysics, 46, 1271-1282.
- MELETTI C., E. PATACCA, and P. SCANDONE (2000). *Construction of a seismotectonic model: the case of Italy*, Pure and Applied Geophysics, 157, 11-35.
- MENON A., T. ORNTHAMMARATH, M. CORIGLIANO, and C.G. LAI (2010). *Probabilistic seismic hazard macrozonation of Tamil Nadu in Southern India*, Bulletin of the Seismological Society of America, 100 (3), 1320-1341.
- NOH, M. (2014). *A parametric estimation of Richter-b and Mmax from an earthquake catalog*, Geosciences Journal, 18(3), 339-345.
- NORIO, O., T. YE, Y. KAJITANI, P. SHI, and H. TATANO (2011). *The 2011 eastern Japan great earthquake disaster: Overview and comments*, International Journal of Disaster Risk Science, 3, 34-42.
- NOWROOZI, A.A. (1976). *Seismotectonic provinces of Iran*, Bulletin of the Seismological Society of America, 66 (4), 1249-1276.
- OH, C.W. (2006). *A new concept on tectonic correlation between Korea, China and Japan: Histories from the late Proterozoic to Cretaceous*, Gondwana Research, 9, 47-61.
- PARK, S.J, and T.-K. HONG (2014). Joint determination of event location and magnitude from historical seismic damage records, Eos Transactions American Geophysical Union, Fall Meeting Supplementary, Abstract S11A-4332.
- PISARENKO, V. F., A. A. LYUBUSHIN, V. B. LYSSENKO, and T. V. GOLUBIEVA (1996). *Statistical estimation of seismic hazard parameters: Maximum possible magnitude and related parameters*, Bulletin of the Seismological Society of America, 86, 691-700.
- POWELL, C.A., G.A. BOLLINGER, M.C. CHAPMAN, M.S. SIBOL, A.C. JOHNSTON, and R.L. WHEELER (1994). *A seismotectonic model for the 300-kilometer-long Eastern Tennessee seismic zone*, Science, 264, 686-688.
- ROBSON, D. S., and J. H. WHITLOCK (1964). *Estimation of a truncation point*, Biometrika, 51, 33-39.
- RYDELEK, P. A., and I. S. SACKS (1989). *Testing the completeness of earthquake catalogues and the hypothesis of self-similarity*, Nature, 337, 251-253.
- SCHOLZ, C.H. (2002). *The mechanics of Earthquakes and Faulting*, second edition, Cambridge University Press, New York, USA, p.471.
- SINGH, M., A. KIJKO, and R. DURRHEIM (2011). *First-order regional seismotectonic models for South Africa*, Natural Hazards 59, 383-400.
- TALWANI, P and J. COX (1985). *Paleoseismic evidence for recurrence of earthquakes near Charleston, South Carolina*, Science, 229, 379-381.
- TATE, R. F. (1959). *Unbiased estimation: Functions of location and scale parameters*, Annals of Mathematical Statistics 30, 341-366.
- TAVAKOLI, B. and M. GHAFORY-ASHTIANY (1999). *Seismic Hazard Assessment of Iran*, Annali Di Geofisica, 42 (6), 1013-1021.
- TINTI, S. and F. MULARGIA (1985). *Effects of magnitude uncertainties on estimating the parameters in the Gutenberg-Richter frequency-magnitude law*, Bulletin of the Seismological Society of America, 75, 1681-1697.
- WIEMER, S., and M. WYSS (2000). *Minimum magnitude of completeness in Earthquake Catalogs: Examples from Alaska, the Western United States, and Japan*, Bulletin of the Seismological Society of America, 90, 859-869.